Supporting Information

Efficient and Stable Inverted MA/Br-Free 2D/3D Perovskite Solar Cells Enabled by *α*-to-*δ* Phase Transition Inhibition and Crystallization Modulation

Zhiyuan Xu,[1,#] Zhihao Guo,[1,#] Haiyun Li,[1,#] Yuqin Zhou,[1] Zhenyu Liu,[4] Ke Wang,[1] Zhijun Li,[1] Huaxin Wang,[1] Saif M. H. Qaid,[2] Omar F. Mohammed,[3] and Zhigang Zang[1,*]

[1]Key Laboratory of Optoelectronic Technology & Systems (Ministry of Education), Chongqing University, Chongqing 400044, China

[2]Department of Physics and Astronomy, College of Sciences, King Saud University, Riyadh, 11451, Kingdom of Saudi Arabia

[3]Advanced Membranes and Porous Materials Center, Division of Physical Science and Engineering, King Abdullah University of Science and Technology, Thuwal, Kingdom of Saudi Arabia.

[4]CDGM Glass Company Limited, Chengdu, Sichuan, China

[#]The authors contributed equally to this work.

*Correspondence Authors: zangzg@cqu.edu.cn (Zhigang Zang)

Experimental Section

Materials

Cesium iodide (CsI), formamidinium iodide (FAI), lead iodide (PbI_2), and PCBM were purchased from Advanced Election Technology Co., Ltd. The nickel nitrate hexahydrate ($Ni(NO_3)_2 \cdot 6H_2O$), sodium hydroxide (NaOH), dimethylformamide (DMF), dimethyl sulfoxide (DMSO), isopropanol (IPA), Chlorobenzene (CB), and Al_2O_3 dispersions were obtained from Sigma Aldrich. [4-(3, 6-dimethyl-9H-carbazol-9-yl)butyl]phosphonic acid (MeO-2PACz) was obtained from TCI America. Bathocuproine (BCP) was purchased from Xi'an Yuri Solar Co., Ltd. Benzyl carbamimidothioate hydrochloride (BLSCl) was obtained from Macklin. All the chemicals and reagents were used directly without further purification.

Preparation of the $Cs_{0.05}FA_{0.95}PbI_3$ perovskite solution

CsI (18.2 mg), FAI (228.7 mg), PbI_2 (645.4 mg), and BLSCl (0.5, 1.0, or 1.5 mg) were dissolved in mixed solutions (DMF: DMSO = 4:1 in volume ratio, 1 mL). The prepared perovskite precursor was stirred for 2 h at ambient temperature before use.

Device fabrication

ITO substrates were sequentially ultrasonic cleaned with suds, DI water, IPA, and absolute ethanol for 15 min, respectively. Before the deposition of the hole transportation layer (HTL), the cleaned ITO/glass substrates were treated with UV-ozone for 30 min. Afterwards, NiO_x NPs dispersion (30 mg mL^{-1} in water) was spin-coated on the substrates at a speed of 5000 rpm for 30 min, followed by annealing at

150 ℃ for 10 min in Air. For the preparation of NiO_x NPs, more preparation details can be found in our previous work.[1] After cooling, the substrates were transferred into the N_2 glovebox. MeO-2PACz solution (0.5 mg mL^{-1} in IPA) was spin-coated on the NiO_x-covered substrates at 3000 rpm for 30 s, followed by thermal annealing at 100 ℃ for 10 min. Then, the Al_2O_3 dispersion solution (0.4 wt% in IPA) was spin-coated on the NiO_x/MeO-2PACz substrates at 5000 rpm for 30 s, followed by thermal annealing at 100 ℃ for 10 min. For the fabrication of perovskite films, a two-step coating procedure was adopted. Briefly, the perovskite precursor containing BLSCl was spin-coated onto the NiO_x/MeO-2PACz/Al_2O_3 substrates at 2000 rpm for 10 s and 4000 rpm for 40 s, and then 150 μL CB was dropped onto the spinning substrates 5 s before the end of the spin coating procedure. The wet films were immediately transferred to the hotplate at 100 ℃ for 30 min. Afterwards, a passivation layer was introduced. Next, PCBM solution (23 mg mL^{-1} in CB) was spin-coated on the perovskite surface at 2500 rpm for 40 s. BCP solution (0.5 mg mL^{-1} in IPA) was spin-coated at 5000 rpm for 30 s. Finally, the 100 nm Ag electrode was thermally evaporated on the top of the devices at a rate of 1.5 Å/s to complete the device.

Characterizations

The *J–V* characteristics of inverted PSCs were measured under 1 sun equivalent illumination in ambient conditions using a Keithley source meter (2400) and the solar simulator, which equipped a 450 W Xenon lamp (Newport 2612 A, Oriel Sol3A). The light intensity was controlled at AM 1.5G (100 mW cm^{-2}) by a standard silicon solar

cell. The exposure area of metal mask in *J–V* measurements was 0.1 cm^2. The external quantum efficiency (EQE) was collected by using a QE-R Solar Cell Spectral Response Measurement System (Enli Technology Co., Ltd., Taiwan). The liquid-state 1H NMR measurements were conducted in d6-DMSO using a Bruker 400 MHz measurement spectrometer. The FTIR spectra were collected by the Nicolet iS50 system of Thermo Fisher Scientific. The XPS spectroscopy was obtained by using the Thermo Scientific ESCALAB 250Xi at Shiyanjia lab (www.Shiyanjia.com). XPS was calibrated using binding energy of C1s (284.80 eV) as the energy standard. In the measured C element spectra, the C-C binding energy position is 284.50 eV, which is 0.3 eV smaller than 284.80 eV. Therefore, all of the examined spectra are selected, and 0.3 eV is added as a whole to complete the XPS results calibration. The UPS measurements were conducted by PHI 5000 Versaprobe at Shiyanjia lab (www.Shiyanjia.com). The GIWAXS measurements were conducted at Beijing Synchrotron Radiation Facility (BSRF), 1W1A station, using X-ray with a wavelength of 1.54792 Å, and the incident angle was 0.2°. Time-of-Flight Secondary Ion Mass Spectrometry (TOF-SIMS) was performed and analyzed by IONTOF M6 instrument with the pulsed primary ions from the ion beam (1 keV) for sputtering. The surface and cross-sectional SEM images were scanned by Zeiss Merlin Compact of Germany. The AFM measurements were conducted by Bruker Dimension Icon (Germany). Contact angle measurement was taken on a JC2000D1 (Shanghai Zhongchen) contact angle instrument. The XRD patterns were collected by Rigaku Ultima IV (Japan). HRTEM analysis was performed

utilizing JEOL JEM 2100F with a probe corrector with accelerating voltage of 100 kV. The HRTEM images were collected using a Gatan K3 direct-detection camera. The active time was established to ensure that the dose rate was below 10 e $Å^{-2}$ s^{-1}, in order to prevent potential beam damage and phase transition of perovskite under the electron beam. The GIXRD patterns were collected by PANalytical Empyrean (Netherlands). The UV-vis absorption spectra were obtained via the Shimadzu UV-3600 spectrometer. Steady-state PL and TRPL were performed by a fluorescence spectrophotometer (FLS1000, Edinburgh Instruments Ltd.) PL mapping was collected via Laser Ramon Instrument (LabRAM HR Evolution). TPC and TPV measurements were conducted using a system excited by a 532 nm (1000 Hz, 6 ns) pulsed laser. The Mott–Schottky and EIS plots were obtained by an electrochemical workstation (CHI 660). The dark J-V characteristic of devices was obtained via the Keithley source meter. All DFT calculations were carried out in the gas phase using Gaussian 16 software package. The slab models were built based on the DFT simulated crystal structures of 3D and BLS-based 2D/3D perovskites. The PBE0 hybrid functional was used along with Los Alamos double-ζ pseudopotential and the associated valence double-ζ basis set. All molecular orbitals were plotted at the isovalue of 0.02.

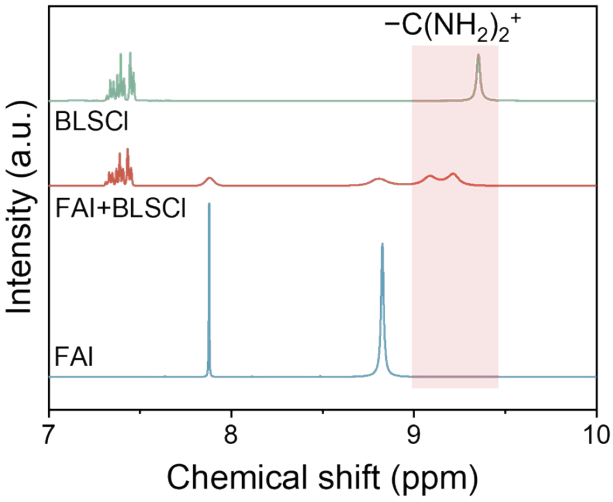

Fig. S1. The amplified 1H-NMR spectra of FAI, BLSCl, and FAI with BLSCl.

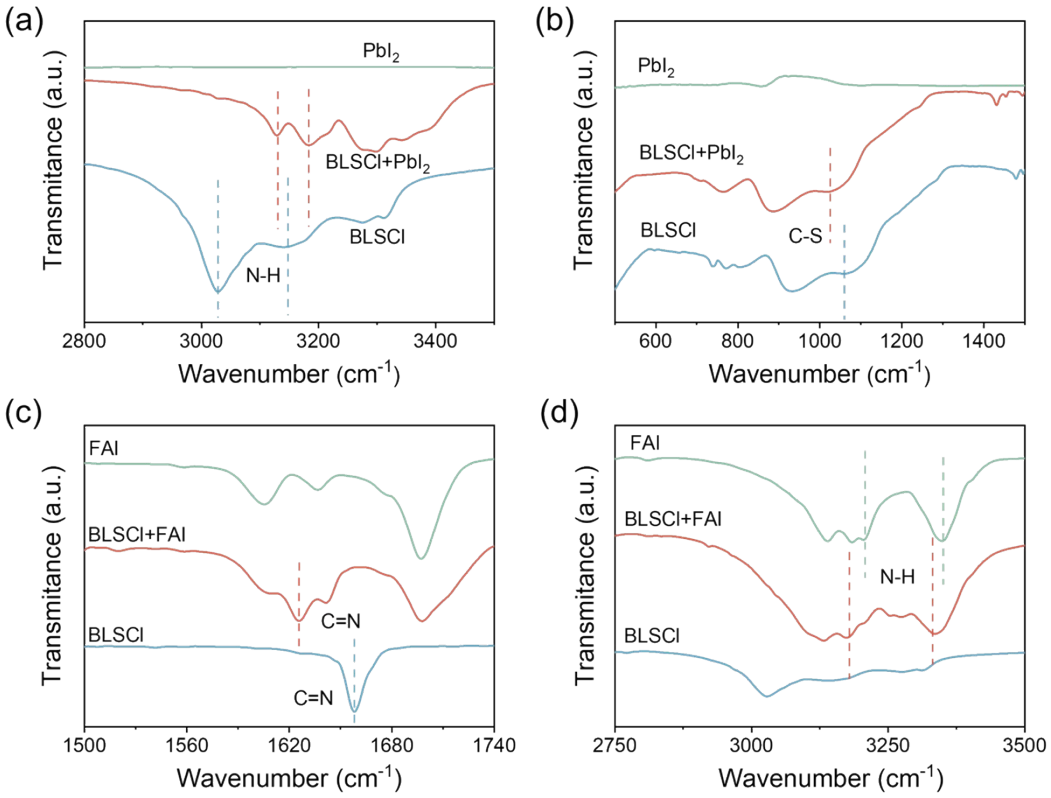

Fig. S2. The amplified FTIR spectra of (a) BLS, PbI_2, and PbI_2 with BLS for N-H stretching peaks, (b) BLS, PbI_2, and PbI_2 with BLS for C-S stretching peaks, (c) BLS, FAI, and FAI with BLS for C=N stretching peaks, and (d) BLS, FAI, and FAI with BLS for N-H stretching peaks.

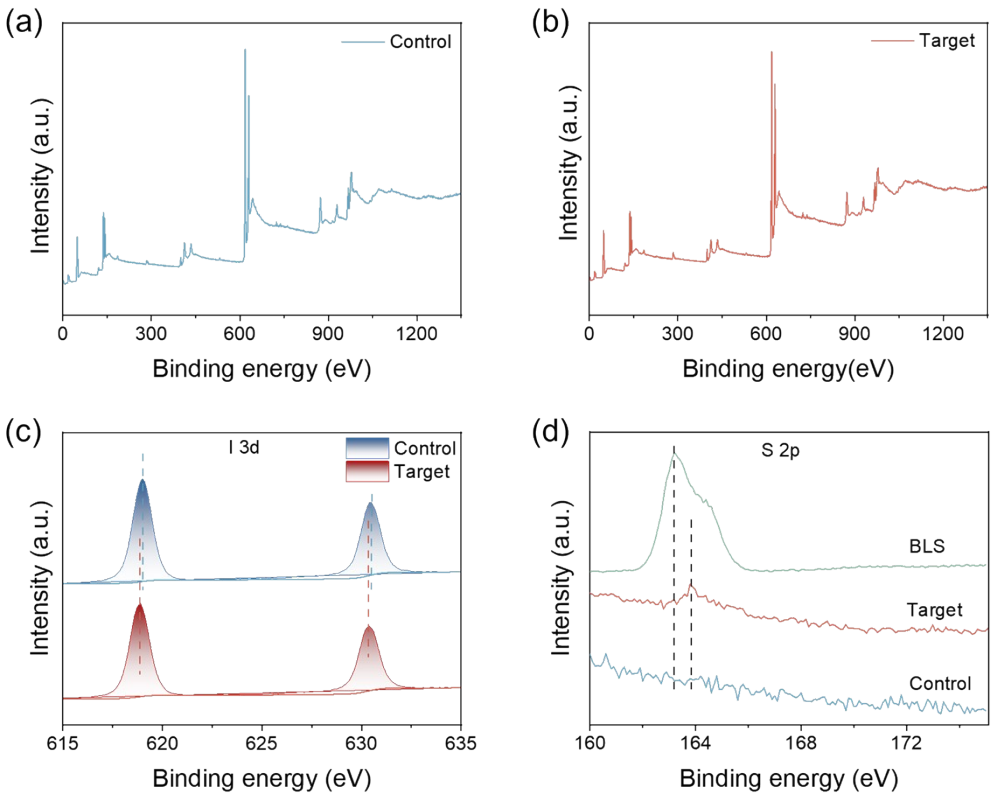

Fig. S3. (a) XPS spectra of control films and (b) XPS spectra of target films. (c) XPS spectra of I 3d of control and target perovskite films. (d) XPS spectra of S 2p for BLS and perovskite films without and with BLS.

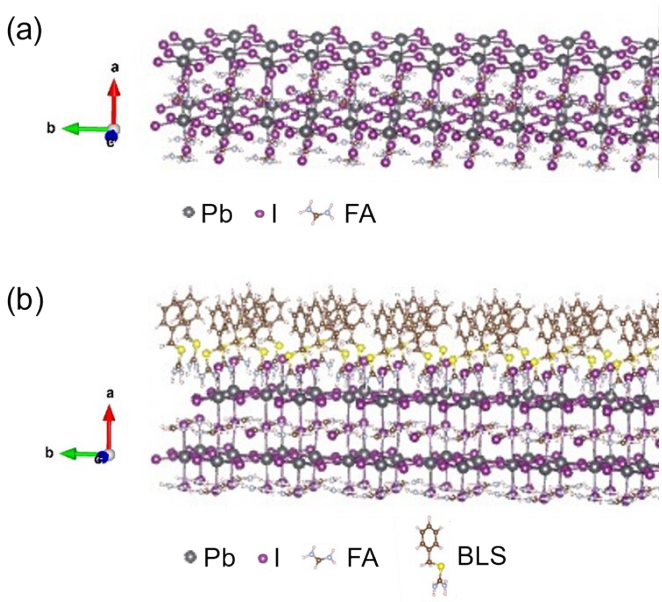

Fig. S4. Theoretical models of (a) 3D perovskites and (b) BLS-based 2D/3D perovskites.

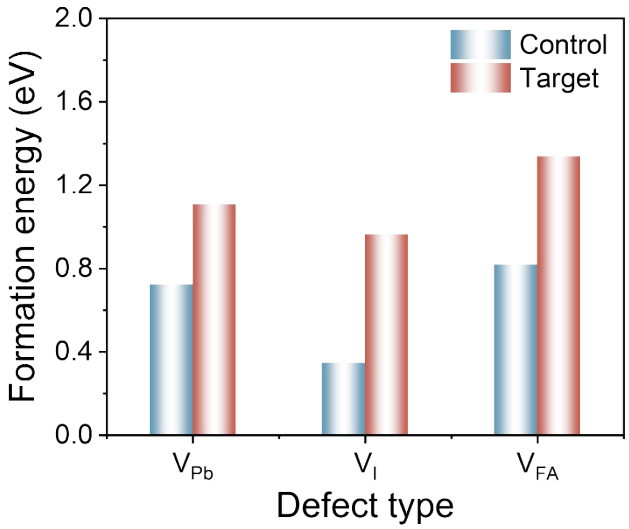

Fig. S5. Defect formation energy of V_{Pb}, V_I and V_{FA} without and with BLS incorporation.

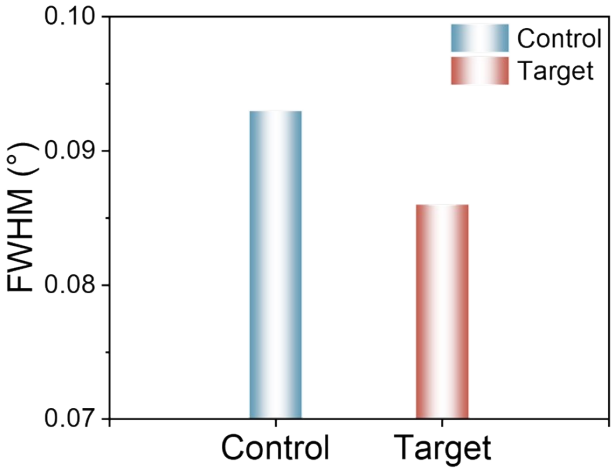

Fig. S6. FWHM of (001) peaks for the control and target perovskite films.

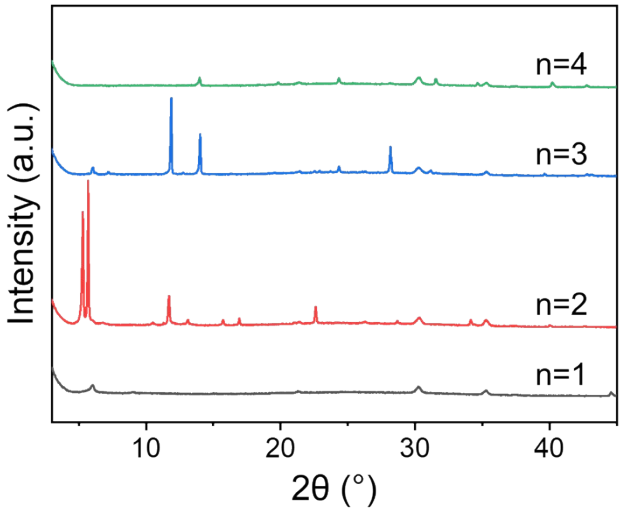

Fig. S7. XRD patterns of the BLS-Pb films with different n values (n = 1-4, without MACl)

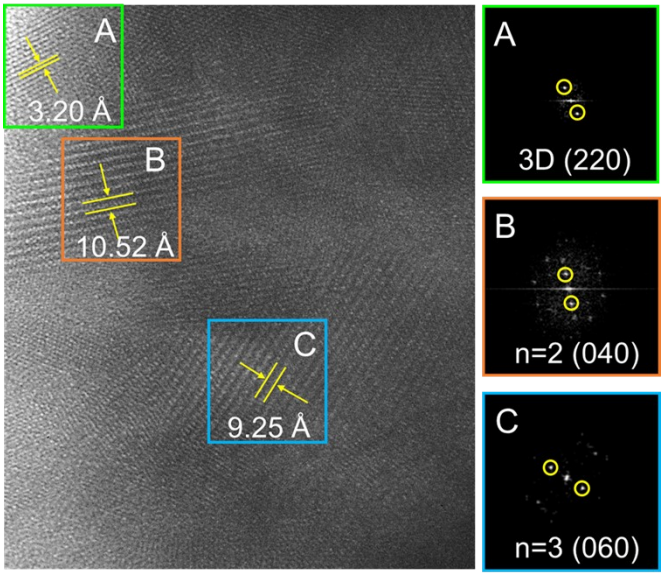

Fig. S8. HRTEM of the target perovskite film and Fast Fourier transforms (FFT) of the of selected area diffraction.

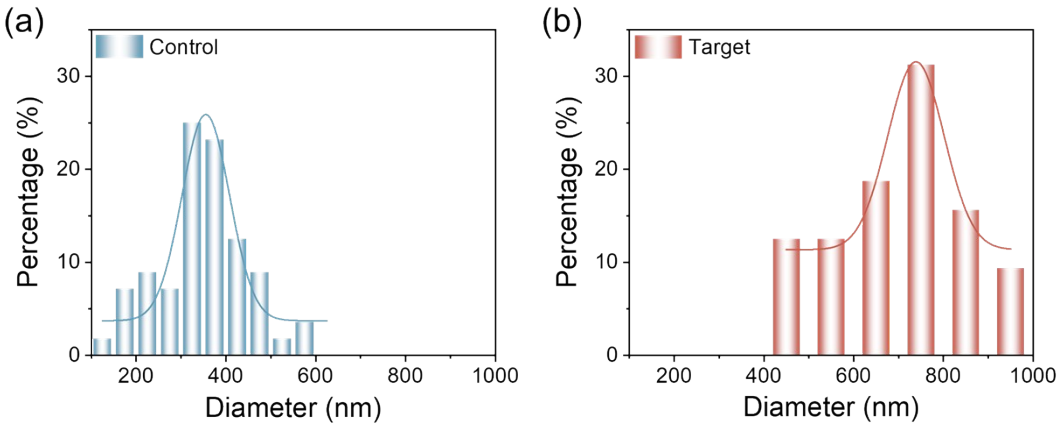

Fig. S9. The corresponding statistical graphic of average grain size for control and target films.

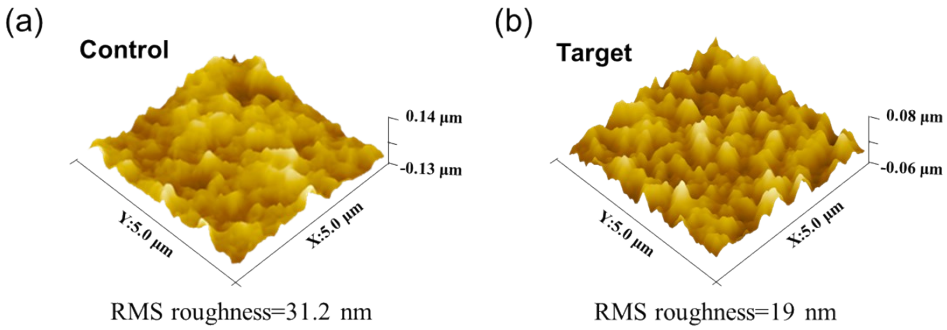

Fig. S10. AFM images of the (a) control and (b) target perovskite films.

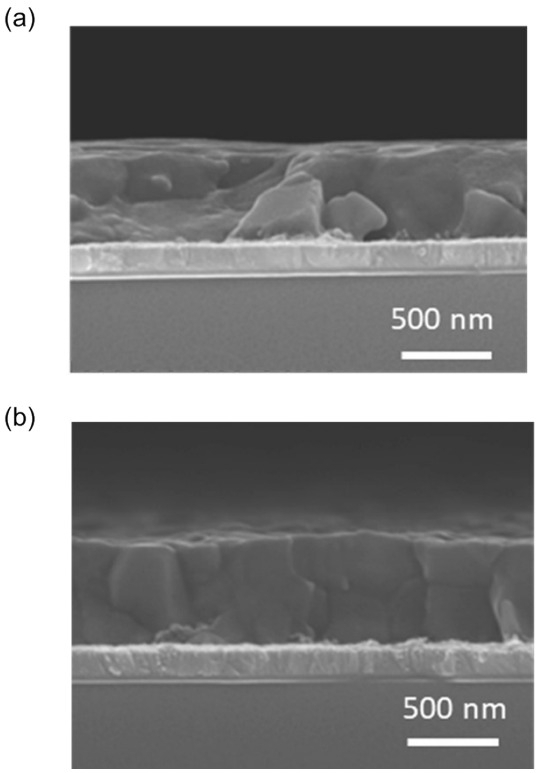

Fig. S11. Cross-sectional SEM images for (a) control and (d) target films.

Fig. S12. Corresponding PL intensity versus annealing time extracted from in-situ PL spectra.

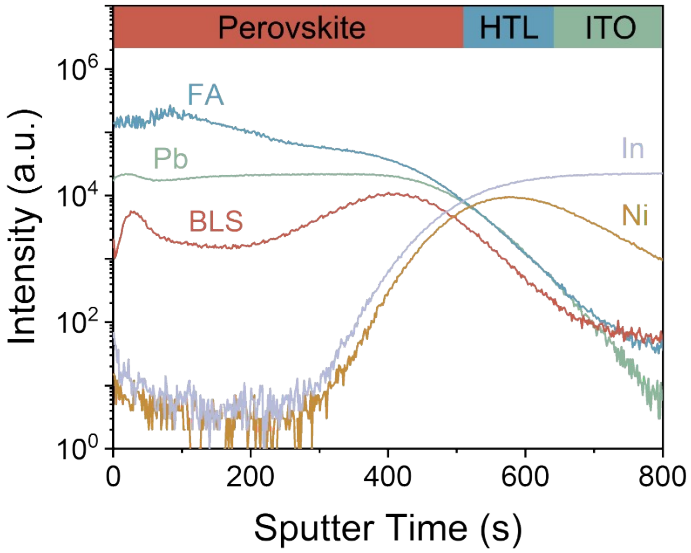

Fig. S13. TOF-SIMS of BLS-incorporated perovskite film deposited on ITO/NiO_x/MeO-2PACz/Al_2O_3 substrates stored under harsh conditions (T = 200 °C, RH = 80%) for 60 min.

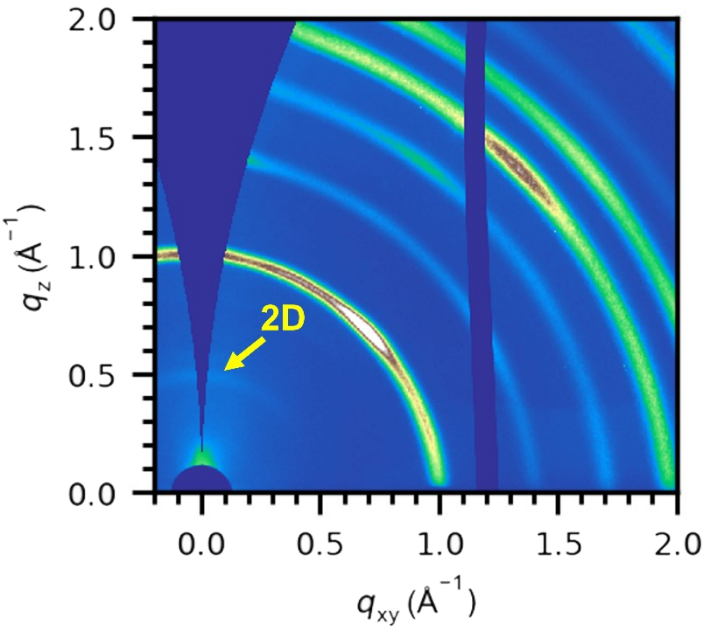

Fig. S14. GIWAXS of BLS-incorporated perovskite film stored under harsh conditions (T = 200 ℃, RH = 80%) for 60 min.

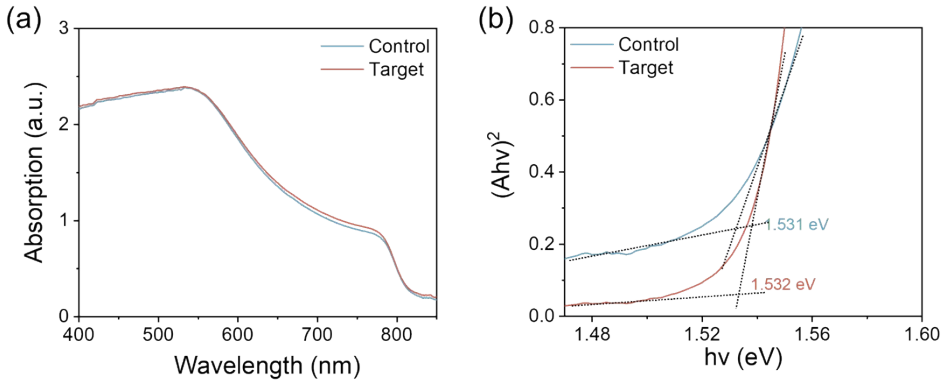

Fig. S15. (a) UV–vis absorption spectra for perovskite films. (b) Tauc plots for perovskite films with/without BLS.

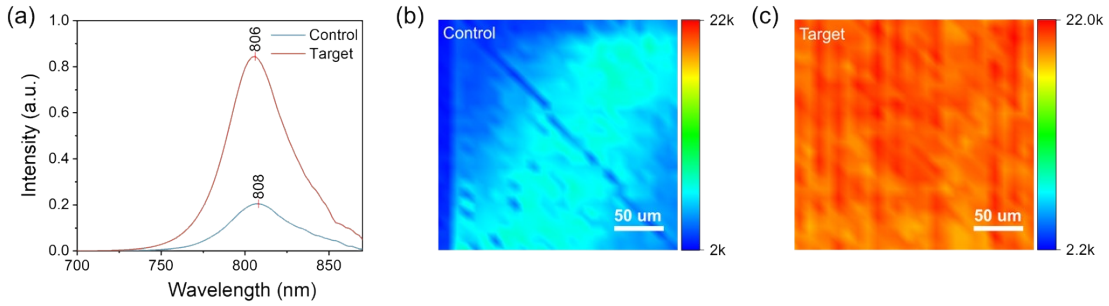

Fig. S16. (a) PL spectra of control and target films. (b) PL mapping of control films. (c) PL mapping of target films.

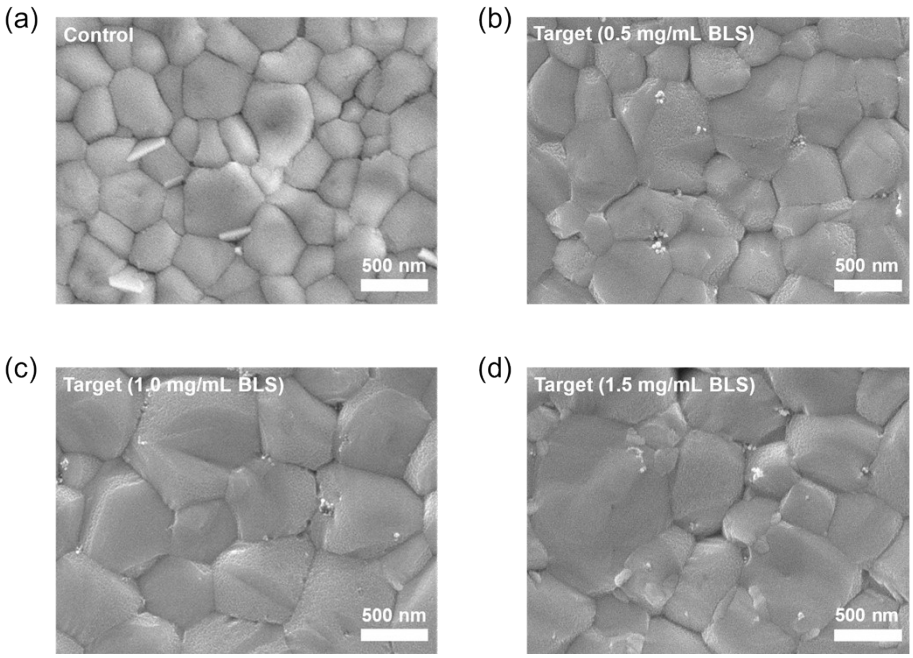

Fig. S17. SEM photos of perovskite films without and with BLS (0.5 mg/mL, 1.0 mg/mL, and 1.5 mg/mL).

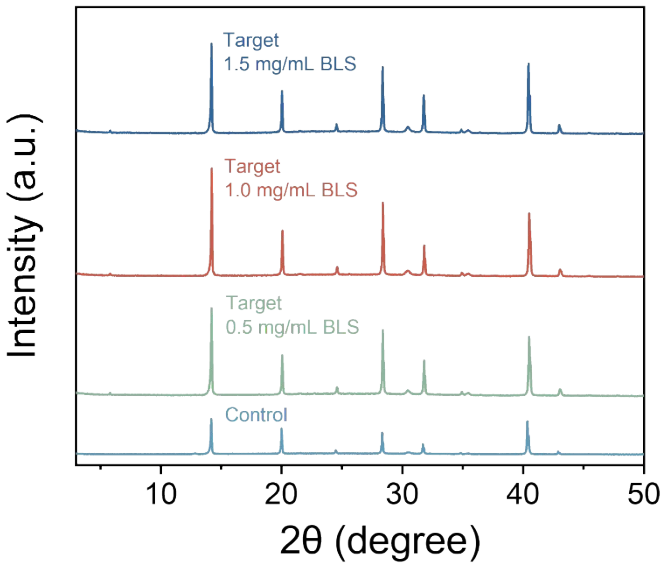

Fig. S18. XRD patterns of perovskite films without and with BLS (0.5 mg/mL, 1.0 mg/mL, and 1.5 mg/mL).

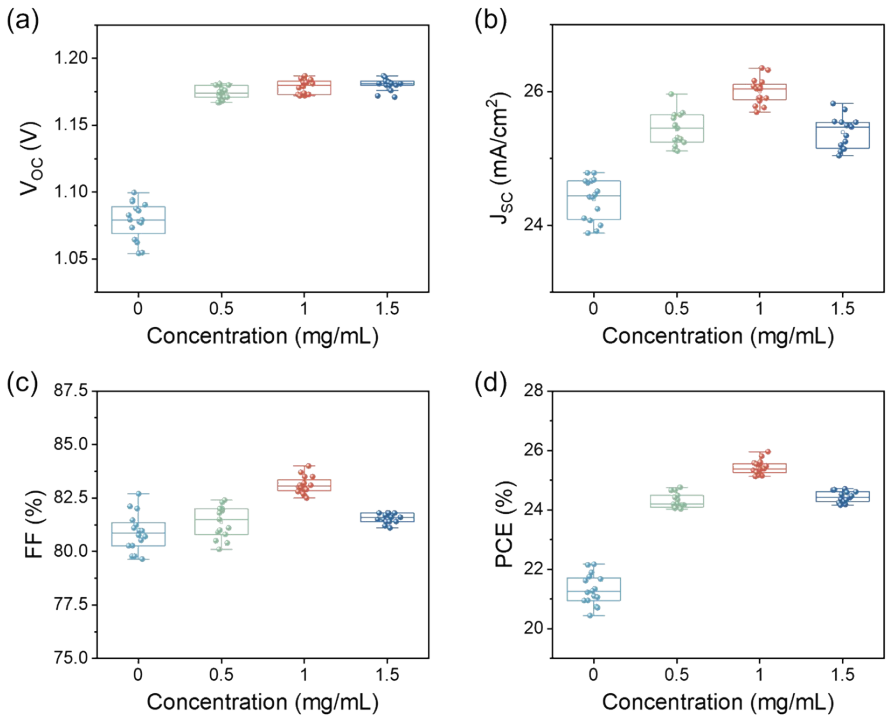

Fig. S19. Statistics of V_{OC}, J_{SC}, FF, and PCE for perovskite devices without and with BLS (0.5 mg/mL, 1.0 mg/mL, and 1.5 mg/mL).

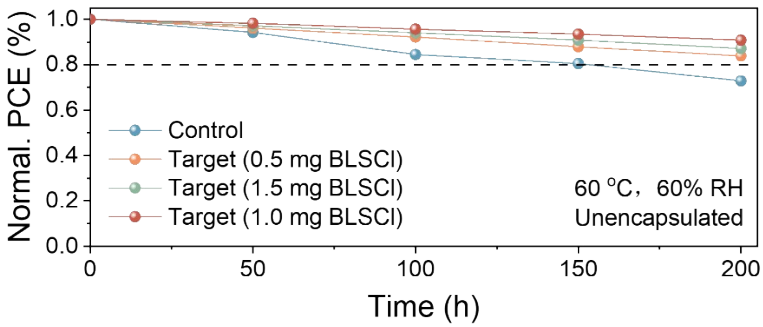

Fig. S20. Stability of perovskite devices without and with BLS (0.5 mg/mL, 1.0 mg/mL, and 1.5mg/mL) at 80 ℃ under 40-50% RH.

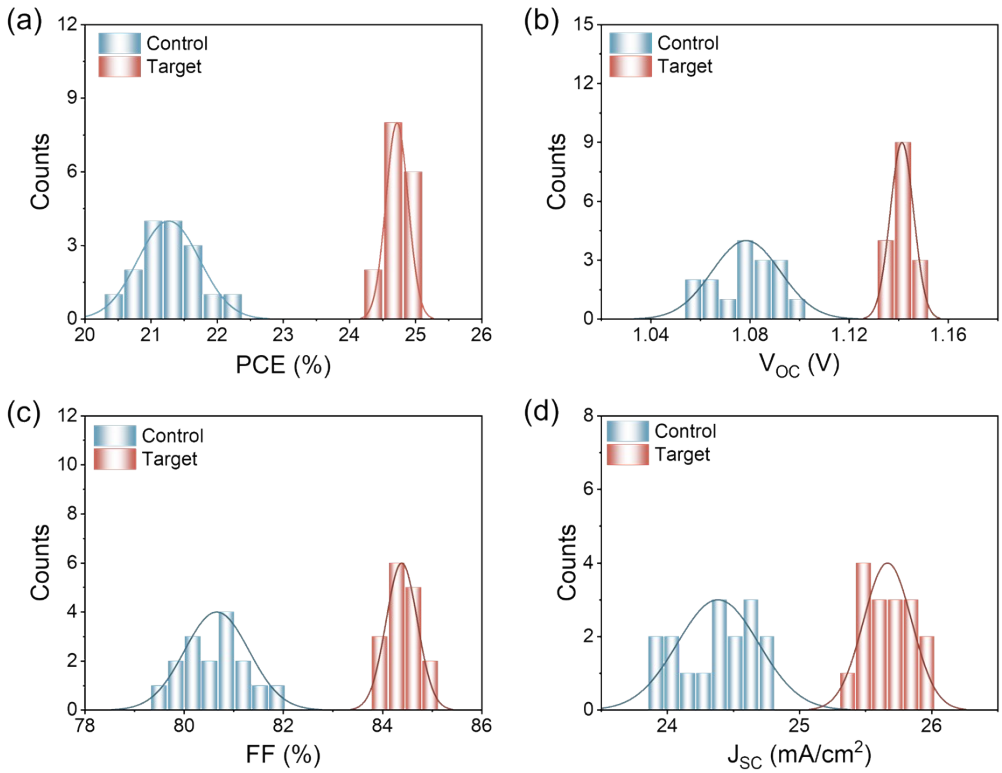

Fig. S21. Statistical box diagram of PV parameters for control and target devices. Each set of data used for the statistical graph has 16 individual devices.

Test and Calibration Center of New Energy Device and Module,
Shanghai Institute of Microsystem and Information Technology,
Chinese Academy of Sciences (SIMIT)

Measurement Report

Report No. 23TR102505

Client Name	Chongqing University
Client Address	No. 174 Shazheng Street, Shapingba District, Chongqing
Sample	Perovskite Solar Cell
Manufacturer	College of Optoelectronic Engineering
Measurement Date	25th October, 2023

Performed by:	Qiang Shi	**Date:** 25/10/2023
Reviewed by:	Wenjie Zhao	**Date:** 25/10/2023
Approved by:	Yucheng Liu	**Date:** 25/10/2023

Address: No.235 Chengbei Road, Jiading, Shanghai **Post Code:**201800
E-mail: solarcell@mail.sim.ac.cn **Tel:** +86-021-69976921

Sample Information

Sample Type	Perovskite solar cell
Serial No.	B6-1#
Lab Internal No.	23102501-6#
Measurement Item	I-V characteristic
Measurement Environment	23.9±2.0°C,41.3±5.0%R.H

Measurement of I-V characteristic

Reference cell	PVM 1121
Reference cell Type	mono-Si, WPVS, calibrated by NREL (Certificate No. ISO 2075)
Calibration Value/Date of Calibration for Reference cell	144.53mA/ Feb. 2023
Measurement Conditions	Standard Test Condition (STC): Spectral Distribution: AM1.5 according to IEC 60904-3 Ed.3, Irradiance: 1000±50W/m^2, Temperature: 25±2°C
Measurement Equipment/ Date of Calibration	AAA Steady State Solar Simulator (YSS-T155-2M) / July.2023 IV test system (ADCMT 6246) / June. 2023 Measuring Microscope (MF-B2017C) / July.2023 SR Measurement system (CEP-25ML-CAS) / April.2023
Measurement Method	I-V Measurement: Logarithmic sweep in both directions (Voc to Isc and Isc to Voc) during one flash based on IEC 60904-1:2020. Spectral Mismatch factor was calculated according to IEC 60904-7 and I-V correction according to IEC 60891.
Measurement Uncertainty	Area: 1.0%(k=2); Isc: 1.9%(k=2); Voc: 1.0%(k=2); Pmax: 2.4%(k=2); Eff: 2.5%(k=2)

Report No. 23TR102505

====Measurement Results ====

	Forward Scan (Isc to Voc)	Reverse Scan (Voc to Isc)
Area	101.09 mm^2	
Isc	25.169 mA	25.141 mA
Voc	1.179 V	1.180 V
Pmax	24.199 mW	24.173 mW
Ipm	23.923 mA	24.073 mA
Vpm	1.012 V	1.004 V
FF	81.57 %	81.51 %
Eff	23.94 %	23.91 %

- Spectral Mismatch Factor: SMM=0.9950.
- Designated illumination area defined by a thin mask was measured by measuring microscope.
- Test results listed in this measurement report refer exclusively to the mentioned measured sample.
- The results apply only at the time of the test, and do not imply future performance.

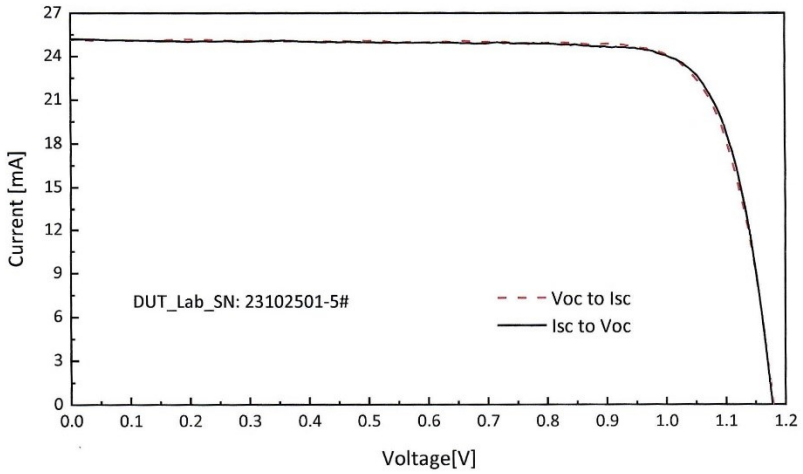

Fig.1 I-V curves of the measured sample

-------End of Report-------

3 / 3

Fig. S22. Certificated results of 1.01 cm^2 device. Independent certification of one of the best-performing target devices by Test and Calibration Center of New Energy Device and Module, Shanghai Institute of Microsystem and Information Technology, Chinese Academy of Sciences (SIMIT).

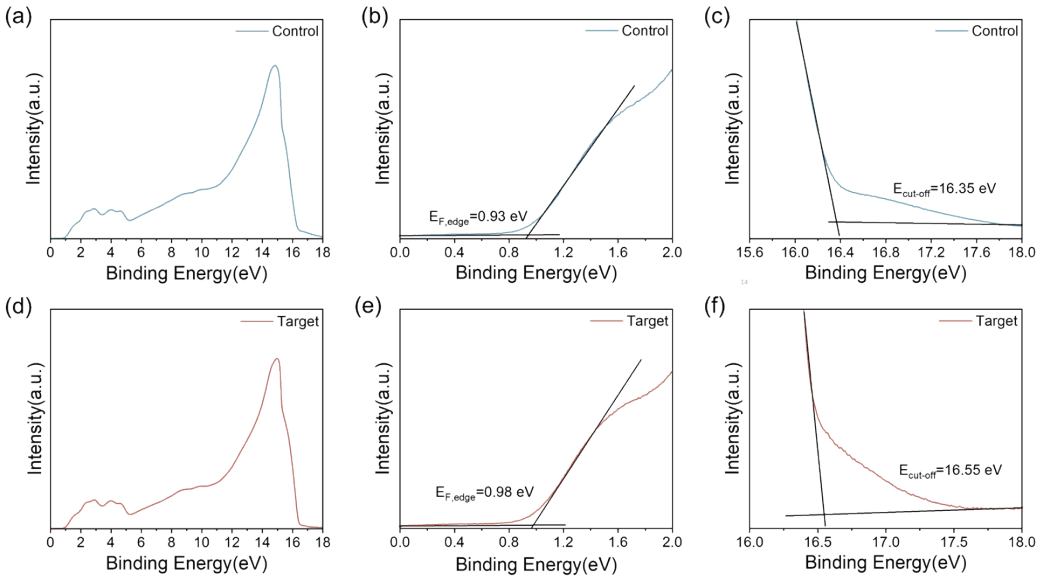

Fig. S23. UPS spectra of (a) full-scale region, (b) cut-off region, and (c) onset region for control perovskite film. UPS spectra of (d) full-scale region, (e) cut-off region, and (f) onset region for target perovskite film.

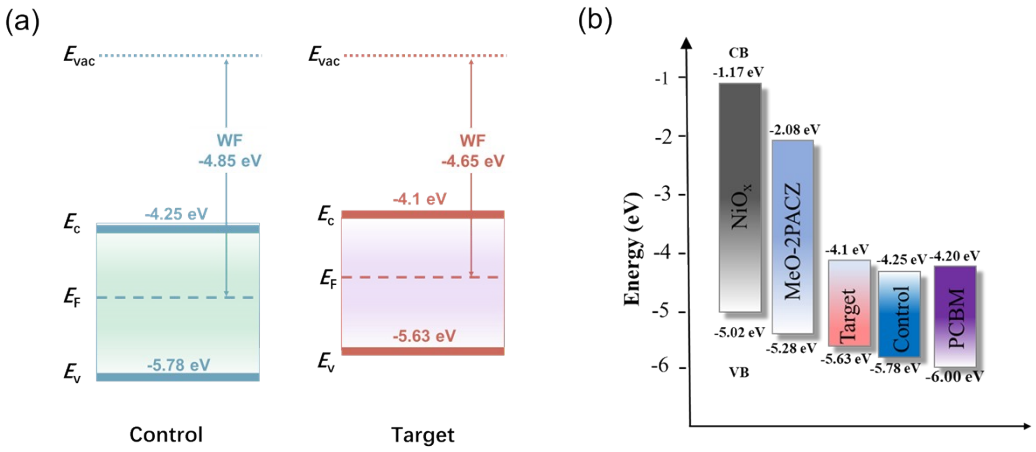

Fig. S24. Band alignment diagram of perovskite film with BLS before and after modification.

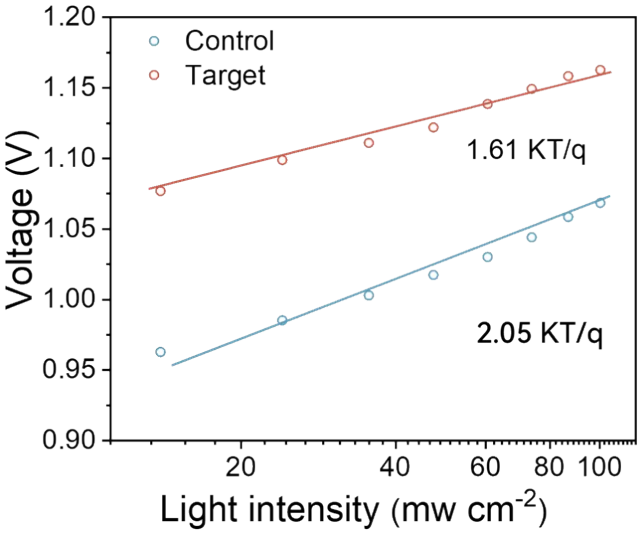

Fig. S25. V_{OC} versus light intensity for the corresponding devices.

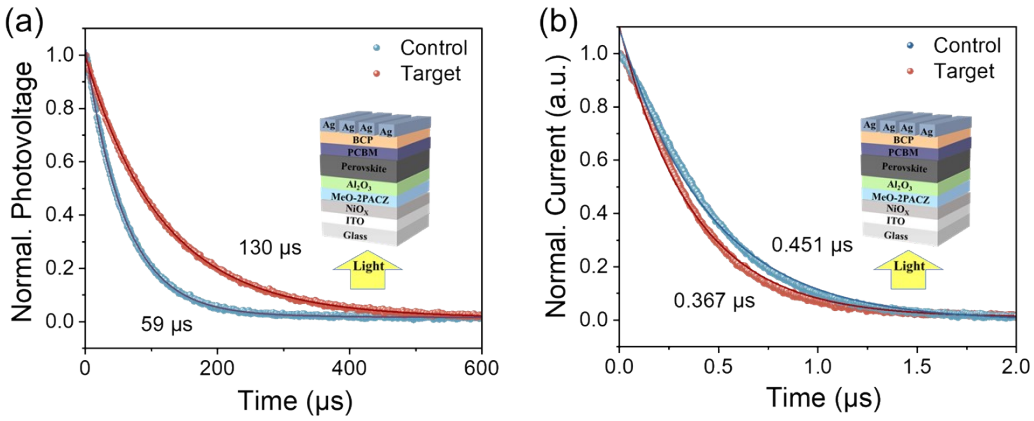

Fig. S26. (a) Transient photovoltage decay curves for control and target perovskite devices. (b) Transient photocurrent decay curves for the control and target devices.

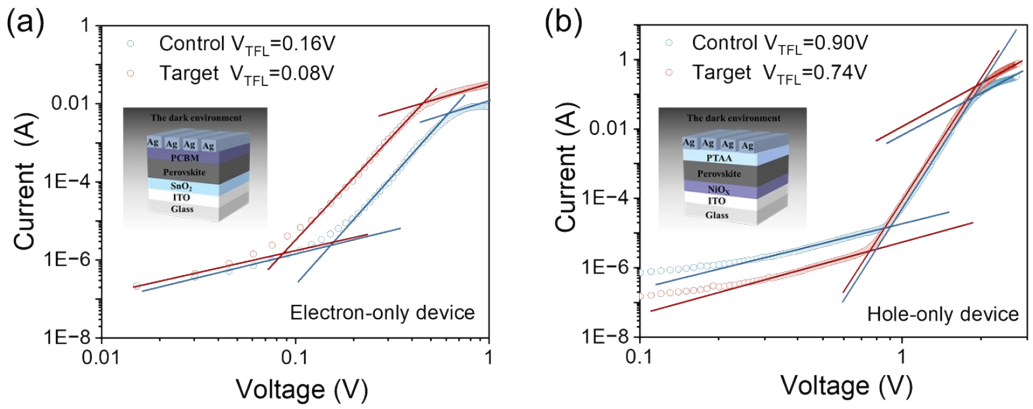

Fig. S27. (a) The I−V curves of the electron-only device. (b) The I−V curves of the hole-only device.

Table S1. Calculated d spacing values for $(BLS)_2FA_{n-1}Pb_nI_{3n+1}$. The values were calculated from X-ray diffraction patterns in Fig. S8 using Bragg`s law.[2]

n=1		**n=2**		**n=3**		**n=4**	
hkl	***d* (Å)**	***hkl***	***d* (Å)**	***hkl***	***d* (Å)**	***hkl***	***d* (Å)**
002	14.68	020	20.96	020	27.54	020	34.12
003	9.82	030	14.18	030	18.64	030	22.94
004	7.26	040	10.51	040	13.81	040	17.26
005	5.92	050	8.21	050	11.32	050	13.73
006	4.96	060	7.02	060	9.25	060	11.41
007	4.24	070	5.99	070	7.89	070	9.82
008	3.67	080	5.28	080	6.92	080	8.58
009	3.29	0100	4.09	090	6.16	090	7.71
0010	2.91	0120	3.52	0100	5.61	0100	6.84
				0120	4.54	0120	5.72

Table S2. The fitted results of TRPL curves for perovskite films. The average lifetime was calculated using the equation $\tau_{ave} = \frac{\sum A_i \tau_i^2}{\sum A_i \tau_i}$.

Samples	τ_1 (ns)	A_1	τ_2 (ns)	A_2	τ_{avg} (ns)
Control	736.41	60.56	1685.89	39.44	1304.68
Target	2153.02	64.14	5730.44	35.86	4290.23

Table S3 Photovoltaic parameters of the PSCs with different BLS concentrations.

Concentrations (mg/mL)		V_{OC} (V)	J_{SC} (mA cm^{-2})	FF (%)	PCE (%)
0	Average	1.078±0.002	24.38±0.09	80.64±0.42	21.28±0.22
	Champion	1.086	24.68	82.71	22.17
0.5	Average	1.174±0.005	25.45±0.24	81.49±0.73	24.29±0.25
	Champion	1.171	25.65	82.40	24.76
1.0	Average	1.178±0.005	26.00±0.10	82.97±0.34	25.46±0.12
	Champion	1.181	26.32	83.50	25.96
1.5	Average	1.181±0.004	25.39±0.24	81.60±0.22	24.43±0.19
	Champion	1.181	25.55	81.80	24.68

Table S4. Photovoltaic parameters of control and target devices.

Device		V_{OC} (V)	J_{SC} (mA cm^{-2})	FF (%)	PCE (%)
Control	Average	1.078±0.002	24.38±0.09	80.64±0.42	21.28±0.22
	Champion	1.086	24.68	82.71	22.17
Target	Average	1.178±0.005	26.00±0.10	82.97±0.34	25.46±0.12
	Champion	1.181	26.32	83.50	25.96

Table S5. The photovoltaic performance of the inverted MA/Br-free FA-based PSC in this work was compared to previous literature that reported PCEs in the area of about 1 cm^2.

Device structure	V_{OC} (V)	J_{SC} (mA cm^{-2})	FF (%)	PCE (%)	Certified PCE (%)	Ref.
ITO/NiO_x/PTAA/Al_2O_3/$Cs_{0.05}FA_{0.95}PbI_3$/ PCBM/BCP/Ag	1.145	25.02	78.1	22.48	--	1
ITO/NiO_x/MeO-2PACz/$FA_{0.84}Cs_{0.12}Rb_{0.04}PbI_3$/$C_{60}$/BCP/Ag	1.166	24.61	76.6	21.47	21.36	3
ITO/NiO_x/PTAA/Al_2O_3/$Cs_{0.05}FA_{0.95}PbI_3$/ PCBM/BCP/Ag	1.144	25.46	75.75	22.06	--	4
ITO/NiO_x/PTAA/Al_2O_3/$Cs_{0.05}FA_{0.95}PbI_3$/ PCBM/BCP/Ag	1.151	25.32	77.12	22.48	--	5
ITO/NiO_x/PTAA/Al_2O_3/$Cs_{0.05}FA_{0.95}PbI_3$/ PCBM/BCP/Ag	1.181	25.71	77.6	23.56	--	6
ITO/NiO_x/PTAA/Al_2O_3/$Cs_{0.05}FA_{0.95}PbI_3$/ PCBM/BCP/Ag	1.190	25.23	80.5	24.17	--	7
ITO/NiO_x/MeO-2PACz/Al_2O_3/$Cs_{0.05}FA_{0.95}PbI_3$/ PCBM/BCP/Ag	**1.191**	**25.82**	**79.8**	**24.54**	**23.94**	**This work**

Table S6. The calculated trap density and mobility for control and target devices.

Device	N_t^e ($\times 10^{15}$) [cm^{-3}]	N_t^h ($\times 10^{15}$) [cm^{-3}]	μ_e ($\times 10^{-3}$) [$cm^3\ V^{-1}\ s^{-1}$]	μ_h ($\times 10^{-3}$) [$cm^3\ V^{-1}\ s^{-1}$]
Control	2.3	1.3	2.66	10.4
Target	1.2	1.1	9.93	7.15

Reference:

1 H. Li, C. Zhang, C. Gong, D. Zhang, H. Zhang, Q. Zhuang, X. Yu, S. Gong, X. Chen, J. Yang, X. Li, R. Li, J. Li, J. Zhou, H. Yang, Q. Lin, J. Chu, M. Grätzel, J. Chen and Z. Zang, *Nat. Energy* 2023, **8**, 946-955.

2 D. Ma, Y. Fu, L. Dang, J. Zhai, I.A. Guzei and S. Jin, *Nano Research* 2017, **10**, 2117-2129.

3 D.B. Khadka, Y. Shirai, M. Yanagida, H. Ota, A. Lyalin, T. Taketsugu and K. Miyano, *Nat. Commun.* 2024, **15**, 882.

4 Q. Zhuang, H. Li, C. Zhang, C. Gong, H. Yang, J. Chen and Z. Zang, *Adv. Mater.* 2023, **35**, 2303275.

5 C. Zhang, H. Li, C. Gong, Q. Zhuang, J. Chen and Z. Zang, *Energy Environ. Sci.* 2023, **16**, 3825-3836.

6 C. Gong, X. Chen, J. Zeng, H. Wang, H. Li, Q. Qian, C. Zhang, Q. Zhuang, X. Yu, S. Gong, H. Yang, B. Xu, J. Chen and Z. Zang, *Adv. Mater.* 2024, **36**, 2307422.

7 C. Gong, H. Li, H. Wang, C. Zhang, Q. Zhuang, A. Wang, Z. Xu, W. Cai, R. Li, X. Li and Z. Zang, *Nat. Commun.* 2024, **15**, 4922.